Micro-drilling of glass fibre reinforced polymer Composites to increase machining ability

1st Dilip G. Gangwani

Ph. D Scholar, Mechanical Engineering Department, Dr. A. P. J. Abdul Kalam University, Indore-452016, M.P., India,

2nd Hardik B. Ramani

Asst. Professor, Mechanical Engineering Department, Dr. A. P. J. Abdul Kalam University, Indore-452016, M.P., India,

Abstract - The de-lamination factor is predicted and evaluated using twist drills, candle stick drills and saw drills in this work. Taguchi's technique and analysis of variance are used in this approach (ANOVA). This research uses an ultrasonic scanning to look at the de-lamination of a carbon fiber-reinforced plastic (CFRP) laminate. The studies were carried out to investigate the de-lamination factor under different cutting circumstances and speed of drill bit. According to the results of the experiments, the feed rate and drill diameter are the two factors that have the greatest impact on overall performance and efficiency. The objective is to compare the effects of feed rate, spindle speed and drill diameter on carbon fiber-reinforced plastic (CFRP) laminate de-lamination. Multivariable linear regression was used to obtain the correlation, which was then compared to the experimental results.

Index Terms – Twist Drill, De-lamination, CFRP, Taguchi's method, ANOVA.

INTRODUCTION

Composite materials provide a number of advantages over traditional materials, including increased specific strength, stiffness, and fatigue properties, which allow for more adaptable structural design. Composite materials' machining practices vary from metal machining in many ways due to their inhomogeneous and anisotropic character. Customer demands have placed a larger emphasis on product development in recent years, posing new obstacles to manufacturers, such as manufacturing techniques. Machining composite materials necessitates a deeper understanding of cutting processes in terms of precision and efficiency. Though near-net form methods have gotten a lot of press, more sophisticated items require further machining to achieve the required accuracy [1]. Drilling is the most commonly used secondary procedure. Fiber-reinforced materials machining Optical inspection of carbon fiber-based composites it's challenging to come up with ways. With the increasing use of Visual inspection and appraisal of composite constructions Interface de-lamination procedures are getting more popular. Ultrasonic scanning has been frequently used in the past [2].

The kinematics of drilling lightweight structures, as well as the hole quality and the impact of welding parameters and tool material, have all been investigated [3]. A de-lamination factor to describe de-lamination in carbon fiber-reinforced plastic drilling (CFRP). Traditional tools, which cut holes in the center and drive chips against walls, generate fibrils or fuzz, which can be considerably minimised [4]. The impact of tool wearing and the subsequent thrust increase was discussed. The complexity of machining two-phase composite materials led to the conclusion that new tools designs as well as various cutting conditions are required. Chip production in composite removal, according to the first, is a process of serial material fractures [5]. It's worth noting that there's a significant link between a rapid rise in cutting temperature and the presence of the critical speed, which causes severe tool wear. The effects of increasing cutting speed on CFRP drilling were investigated. Based on their physical and mechanical qualities, distinct tool wear in cutting CFRP and GFRP was compared and the effect of processing variables on drilling damage was explored [6]. An intelligent machining system for determining critical process parameters and designing a new machine tool for diverse cutting circumstances [7]. A general overview of the numerous machining options for composites can be found here [1]. Drilling induced de-lamination occurs on both the workpiece's entrance and exit planes. Researchers have looked at examples where de-lamination in drilling has been linked to the thrust force during the drill's exit, both analytically and empirically [8]. As has been demonstrated, the chisel edge is responsible for a significant percentage of the thrust force. The thrust force increases when the chisel edge length is increased [9]. A smaller piece of the last laminate bends because the candle stick and saw drills have a smaller centre than the twist drill. Experiments show that there is a critical thrust force below which delamination does not occur [10]. Interface de-lamination growing from the crack points causes matrix cracks above that level. The first mathematical model for determining the twist drill's critical thrust force was developed [11]. They used linear elastic fracture mechanics to find the critical thrust force, which is related to drilling parameters and composite material properties in composite laminate delamination [12]. For linking the thrust force with the commencement of de-lamination, a series of analytical models of particular drills (candle stick drill, saw drill, core drill and step drill) were developed [13]. To get the best drilling settings for De-lamination-free drilling in composite laminates, a method integrating Taguchi's method with a multi-objective optimization criterion was developed. A similar methodology was presented, which used Taguchi's method and analysis of variance (ANOVA) to demonstrate a correlation between cutting velocity and feed rate and CFRP laminate de-lamination [14]. The usage of various drill bits and the characterization of their machinability were rarely considered in design experiments, despite the fact that all of the preceding work adds to the practice of twist drilling [15]. The de-lamination parameters of twist drills, candle stick drills and saw drills are predicted and compared in this article [16].

EXPERIMENTAL PROCEDURE

I. Specimens and drilling tests

Autoclave moulding was used to create composite materials for drilling from a woven fabric carbon fiber/epoxy matrix. The CFRP laminates were about 5 mm thick. A vertical drill machine was used to cut specimens measuring 200mm x 30mm. As illustrated in Fig. 1, drilling experiments were performed on a vertical machining center. To support the laminate, which is firmly held on top of the dynamometer, an appropriate fixture with a central hole of 24 mm diameter was employed. As illustrated in Fig. 2, all three drill bits were made of high-speed steel with a 30^0 helix angle and a 10 mm diameter.

II. Taguchi method

Taguchi methods, which combine experiment design theory and the concept of a quality loss function, have been used to the resilient design of products and processes, and have solved numerous perplexing industrial challenges [17]. Three elements, each at three levels, are studied in order to observe the degree of influence of control factors (feed rate, spindle speed and drill diameter) in drilling. The drilling test parameters are listed in Table 1.

III. Ultrasonic C-Scan

De-lamination is one of the most serious concerns when drilling fiber-reinforced composite materials, and assessing drilling-induced de-lamination damage in the material is difficult, especially for carbon fiber-based composites, which are tough to evaluate visually. Visualizing and evaluating internal de-lamination is a tough and time-consuming task. It is extremely desirable to nondestructively interrogate composite materials to acquire comprehensive knowledge of the size, shape and location of de-lamination.

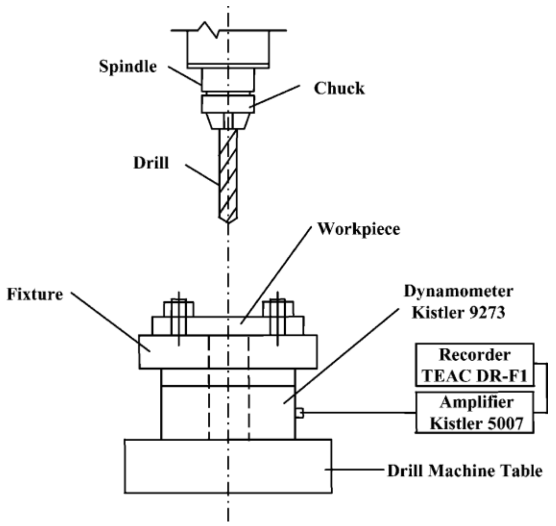

Fig. 1. Schematic of Vertical Drilling Machine

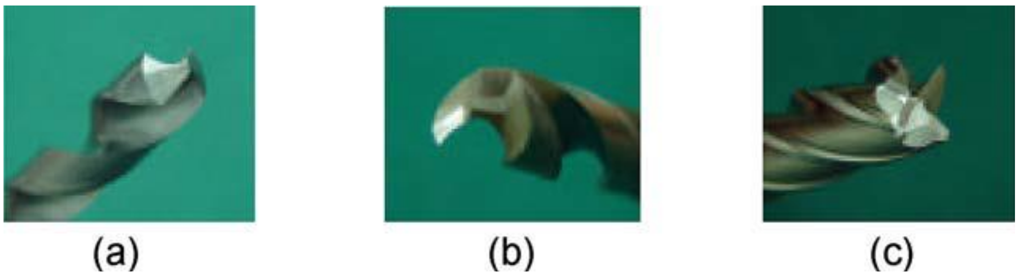

Fig. 2. Three distinct types of drills are shown in this photograph.

(a) Twist drill, (b) candle stick drill, (c) saw drill.

Sample	Parameter	Level 1	Level 2	Level 3
A	Feed rate (mm/rev)	0.01	0.02	0.03
B	Spindle speed (rpm)	800	900	1000
C	Drill diameter (mm)	6	8	10

Table 1: Levels of drill test parameters

The current work describes an ultrasonic scan that uses sound energy at frequencies above 20 kHz to detect specimen defects. A focused broadband transducer (3.1 mm diameter, 17 mm focal length) with a centre frequency of 7 MHz was utilised to scan the tested specimens immersed in water at normal incidence in pulse-echo mode. A scanning bridge with a resolution of 0.025 mm, an ultrasonic pulse receiver, and a digital oscilloscope for acquiring radio frequency echo signals make up the testing device. For all post-processing data for de-lamination reconstruction, the same gate location and width were chosen. Figure 3 depicts an ultrasonic scan scheme.

CALCULATION OF DE-LAMINATION FACTOR

The ultrasonic image data is converted into a grey level array throughout the imaging process. The de-lamination factor is calculated using these values. Each scanning produced a picture with a resolution of 125 X 125 pixels (pixels). Each de-lamination image is represented by an array of grey scale values (0–256) that correlate to laminate density changes. When the pixel value of the centre drilled hole exceeds the threshold value, it is set to 0 (black) to produce the useable image; the de-lamination zone is set to 255 in the meantime (white). As shown in Fig. 4, the suitable threshold values were found by looking at the histogram of array values and comparing them to the original and binary images. The ratio of the maximum diameter (Dmax) of the de-lamination zone to the hole diameter determines the drilling de-lamination factor based on binary images (D). Figure 5 depicts the scheme. The value of the de-lamination factor (Fd) is as follows:

$$F_D = \frac{D_{max}}{D} \quad \ldots(1)$$

Where the unit of D_{max} and D is the pixel.

EXPERIMENTAL RESULTS

I. Analysis of variance

The findings of the de-lamination factor of three drilling sets obtained by Eq. 2 are shown in Table 2. (1). The findings of the ANOVA with the de-lamination factor in CFRP laminate are shown in Tables 3–5. The feed rate (P=80.9 percent) is the most important variable impacting the de-lamination factor in Table 3. In twist drilling CFRP laminate, the feed rate has statistical and physical relevance. Drill diameter (P=60.6 percent) has statistical and physical significance on the de-lamination factor produced, according to Table 4. The feed rate component (P=25.9%) has no statistical significance when it comes to the de-lamination factor.

Table 5 shows the statistical and physical significance of feed rate, spindle speed, and drill diameter on the de-lamination factor achieved. According to the results of the investigation, the feed rate and drill diameter have the greatest impact on overall performance [18]. Proposed the models to describe the benefits of dispersing thrust force toward the drill periphery, as demonstrated by the saw drill and candle stick drill [19].

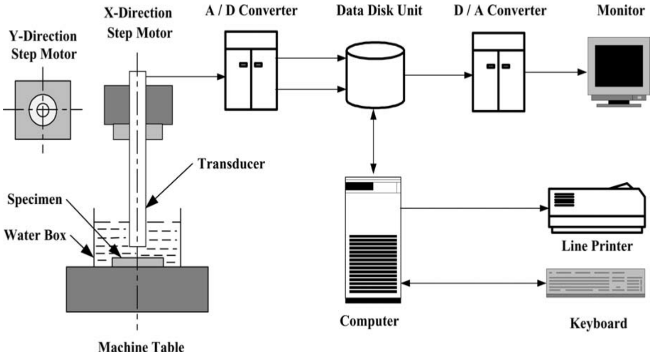

Fig. 3. Flow Process chart of ultrasonic scanning

Trail	A	B	C	De-lamination factor (F_d)		
	1	2	3	Twist drill	Candle stick drill	Saw drill
1	0.01	801	6	1.667	1.396	1.417
2	0.01	1001	8	1.531	1.375	1.313
3	0.01	1201	10	1.475	1.350	1.350
4	0.02	801	6	1.375	1.344	1.328
5	0.02	1001	8	1.375	1.300	1.288
6	0.02	1201	10	1.333	1.396	1.396
7	0.03	801	6	1.313	1.313	1.288
8	0.03	1001	8	1.375	1.375	1.292
9	0.03	1201	10	1.328	1.297	1.297

Table 2. Orthogonal array and values of de-lamination factor (F_d)

Factor	Level (S/N)			DF	SS	V	P(%)
	1	2	3				
A	-3.85	-2.67	-2.53	2	3.08	1.54	80.9
B	-3.18	-3.07	-2.78	2	0.27	0.14	
C	-3.22	-2.97	-2.83	2	0.24	0.12	
Error				2	0.21	0.11	
PE				6	0.72	0.12	19.1
Total				8	3.80		100

Where,

DF is a degree of freedom,

SS is a sum of squares,

P is a percentage of contribution,

PE is a pooled error.

Table 3. ANOVA for the de-lamination factor (F_d) of twist drill

Factor	Level (S/N)			DF	SS	V	P(%)
	1	2	3				
A	-2.76	-2.58	-2.46	2	0.12	0.065	25.9
B	-2.61	-2.60	-2.59	2	0	0	
C	-2.85	-2.53	-2.42	2	0.31	0.155	60.6
Error				2	0.06	0.034	13.3
PE				4	0.06	0.017	13.4
Total				8	0.52		100

Table 4. ANOVA for the de-lamination factor (F_d) of Candle stick drill

Factor	Level (S/N)			DF	SS	V	P(%)
	1	2	3				
A	-2.66	-2.52	-2.23	2	0.30	0.15	38.6
B	-2.56	-2.26	-2.59	2	0.20	0.10	25.5
C	-2.72	-2.36	-2.33	2	0.27	0.135	35.0
Error				2	0.01	0.005	0.9
PE				2	0.01	0.005	
Total				8	0.78		100

Table 5. ANOVA for the de-lamination factor (F_d) of saw drill

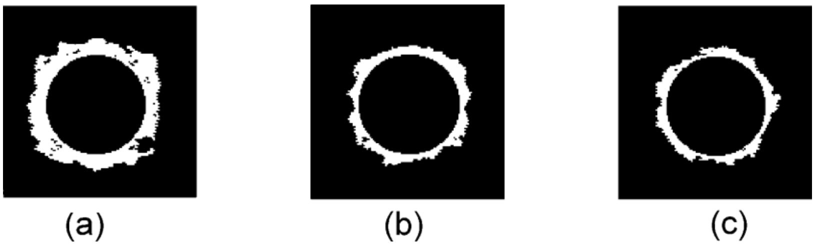

Fig 4. Ultrasonic scanner shows the extent of drilling-induced in de-lamination for different drills (f= 0.01 mm/rev, N= 1000 rpm and d= 8 mm).

(a) Twist drill, (b) candle stick drill, (c) saw drill.

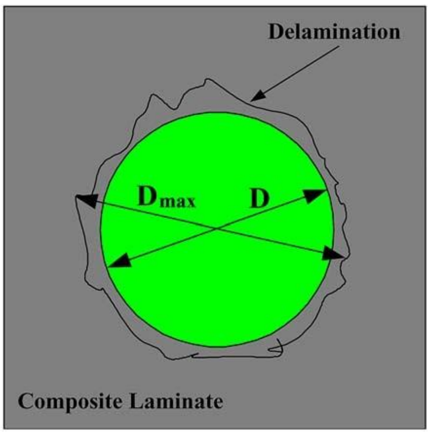

Fig. 5. Graphical view of de-lamination factor in ultrasonic scanner equipment.

II. Correlation between de-lamination factor and cutting parameters

The association between de-lamination factor and cutting parameters in drilling CFRP was discovered using multi-variable linear regression analysis [20]. The following are possible expressions for the equations:

Type of drill	Test	f (mm/rev)	N (rpm)	d (mm)
Twist drill	1	0.026	1101	6.7
	2	0.014	901	8.5
Candle stick drill	3	0.026	1101	6.7
	4	0.014	901	8.4
Saw drill	5	0.026	1101	6
	6	0.014	901	8

Table 6: Cutting conditions in confirmation tests

Test	De-lamination factor (F_d)		
	Experimental values	Model Eqs. (2) and (4)	Error (%)
1	1.324	1.368	3.3
2	1.382	1.484	7.3
3	1.287	1.358	5.5
4	1.324	1.353	2.2
5	1.354	1.342	0.9
6	1.359	1.345	1.0

Table 7: Experimental confirmation and comparison with model

(A) Twist drill

$$F_d = 1.961 - 10.955f - 1.81 \times 10^{-4} N - 1.77 \times 10^{-2} d \qquad R^2 = 0.796 \qquad \ldots(2)$$

(B) Candle stick drill

$$F_d = 1.539 - 2.274f - 7.81 \times 10^{-6} N - 1.77 \times 10^{-2} d$$
$$R^2 = 0.824 \qquad \ldots(3)$$

(C) Saw drill

$$F_d = 1.508 - 3.385f + 8.681 \times 10^{-6} N - 1.49 \times 10^{-2} d \qquad R^2 = 0.654 \qquad \ldots(4)$$

Where

‘f’ is the feed rate in mm/rev,

‘N’ is the spindle speed in rpm and

‘d’ is the drill diameter in mm.

III. Confirmation test

Table 6 shows the cutting conditions utilised in the confirmation testing. Table 7 shows the contrast between the predicted values of the models created in this work and the de-lamination factor experimental data. Both experimental results and model results (Eqs. (2)–(4)) exhibit the same deviation (within 8 percent). As a result, Eqs. (2)–(4) are shown to be a realistic and practical method for determining the drilling-induced de-lamination factor.

CONCLUSIONS

This work employed design experiments to provide an experimental approach to evaluating de-lamination produced by various drill bits. The following is a summary of the findings:

1. The feed rate and drill diameter are thought to be the most important factors in overall performance.

2. The de-lamination factor is lower with the candle stick and saw drills than with the twist drill. The findings are consistent with previous industrial experience.

3. The confirmation tests revealed a feasible and effective approach for determining the drilling induced de-lamination factor (errors of less than 8%) in composite material drilling.

ACKNOWLEDGEMENTS

This work is supported by the workshop of Dr. A. P. J. Abdul Kalam University. I am thankful to the workshop Superintendent and its team member for their support to make my research proper and fluent with all machining equipments.

REFERENCES

[1] W. Vanderlinden, P. J. Kolbeck, F. Kriegel, P. U. Walker, and J. Lipfert, “A benchmark data set for the mechanical properties of double-stranded DNA and RNA under torsional constraint,” *Data Br.*, vol. 30, p. 105404, 2020, doi: 10.1016/j.dib.2020.105404.

[2] N. H. Mohammed and D. W. Wolla, “Optimization of machining parameters in drilling hybrid sisal-cotton fiber reinforced polyester composites,” *AIMS Mater. Sci.*, vol. 9, no. 1, pp. 119–134, 2022, doi: 10.3934/matersci.2022008.

[3] O. Isbilir and E. Ghassemieh, “Finite element analysis of drilling of carbon fibre reinforced composites,” *Appl. Compos. Mater.*, vol. 19, no. 3–4, pp. 637–656, 2012, doi: 10.1007/s10443-011-9224-9.

[4] S. Jayabal and U. Natarajan, “Drilling analysis of coir-fibre-reinforced polyester composites,” *Bull. Mater. Sci.*, vol. 34, no. 7, pp. 1563–1567, 2011, doi: 10.1007/s12034-011-0359-y.

[5] E. Brinksmeier, S. Fangmann, and R. Rentsch, “Drilling of composites and resulting surface integrity,” *CIRP Ann. - Manuf. Technol.*, vol. 60, no. 1, pp. 57–60, 2011, doi: 10.1016/j.cirp.2011.03.077.

[6] R. S. Anand and K. Patra, “Mechanistic cutting force modelling for micro-drilling of CFRP composite laminates,” *CIRP J. Manuf. Sci. Technol.*, vol. 16, pp. 55–63, 2017, doi: 10.1016/j.cirpj.2016.07.002.

[7] J. P. Davim and P. Reis, “Study of delamination in drilling carbon fiber reinforced plastics (CFRP) using design experiments,” *Compos. Struct.*, vol. 59, no. 4, pp. 481–487, 2003, doi: 10.1016/S0263-8223(02)00257-X.

[8] M. Ghahramani, R. Yousefi, K. Khoshaman, S. S. Moghadam, and B. Kurganov, “Analysis of the data on titration of native and peroxynitrite modified αA- and αB-crystallins by Cu2+-ions,” *Data Br.*, vol. 30, p. 105492, 2020, doi: 10.1016/j.dib.2020.105492.

[9] E. T. Akinlabi, A. S. Osinubi, N. Madushele, S. A. Akinlabi, and O. M. Ikumapayi, “Data on microhardness and structural analysis of friction stir spot welded lap joints of AA5083-H116,” *Data Br.*, vol. 33, p. 106585, 2020, doi: 10.1016/j.dib.2020.106585.

[10] M. Palmer, M. Masikini, L. W. Jiang, J. J. Wang, F. Cummings, and M. Chowdhury, “Dataset of N-doped CuO:NiO mixed oxide thin film sensor for glucose oxidation,” *Data Br.*, vol. 33, p. 106408, 2020, doi: 10.1016/j.dib.2020.106408.

[11] S. Datta and T. Limpanuparb, “Geometric and energetic data from quantum chemical calculations of halobenzenes and xylenes,” *Data Br.*, vol. 30, p. 105386, 2020, doi: 10.1016/j.dib.2020.105386.

[12] C. Guo, J. Qian, and D. Reynaerts, “Electrochemical Machining with Scanning Micro Electrochemical Flow Cell (SMEFC),” *J. Mater. Process. Technol.*, vol. 247, pp. 171–183, 2017, doi: 10.1016/j.jmatprotec.2017.04.017.

[13] G. Q. Wang, H. S. Li, N. S. Qu, and D. Zhu, "Investigation of the hole-formation process during double-sided through-mask electrochemical machining," *J. Mater. Process. Technol.*, vol. 234, pp. 95–101, 2016, doi: 10.1016/j.jmatprotec.2016.01.010.

[14] T. Sathish, "Experimental investigation of machined hole and optimization of machining parameters using electrochemical machining," *J. Mater. Res. Technol.*, vol. 8, no. 5, pp. 4354–4363, 2019, doi: 10.1016/j.jmrt.2019.07.046.

[15] G. Rajamurugan, A. P. Sanjay, P. Krishnasamy, B. Muralidharan, and S. Jain, "Drilling and mechanical performance analysis on flax-sisal hybrid composite embedded with perforated aluminum foil," *J. Reinf. Plast. Compos.*, vol. 39, no. 23–24, pp. 902–917, 2020, doi: 10.1177/0731684420937070.

[16] J. W. Kim, J. Nam, J. Jeon, and S. W. Lee, "A Study on Machining Performances of Micro-Drilling of Multi-Directional Carbon Fiber Reinforced Plastic," *Materials (Basel).*, vol. 14, p. 685, 2021.

[17] S. Aravind, K. Shunmugesh, J. Biju, and J. K. Vijayan, "Optimization of Micro-Drilling Parameters by Taguchi Grey Relational Analysis," *Mater. Today Proc.*, vol. 4, no. 2, pp. 4188–4195, 2017, doi: 10.1016/j.matpr.2017.02.121.

[18] A. Bhardwaj *et al.*, "To study the effect of drilling process parameters on glass fiber reinforced composite," *Mater. Today Proc.*, vol. 26, no. xxxx, pp. 2333–2336, 2019, doi: 10.1016/j.matpr.2020.02.502.

[19] C. C. Tsao and H. Hocheng, "Taguchi analysis of delamination associated with various drill bits in drilling of composite material," *Int. J. Mach. Tools Manuf.*, vol. 44, no. 10, pp. 1085–1090, 2004, doi: 10.1016/j.ijmachtools.2004.02.019.

[20] S. A. Sobri, R. Heinemann, and D. Whitehead, "Sequential laser–mechanical drilling of thick carbon fibre reinforced polymer composites (Cfrp) for industrial applications," *Polymers (Basel).*, vol. 13, no. 13, 2021, doi: 10.3390/polym13132136.